Chapter

Nonstoichiometry Role on the Properties of Quantum-Paraelectric Ceramics

Alexander Tkach and Paula M. Vilarinho

Abstract

Among the lead-free perovskite-structure materials, strontium titanate ($SrTiO_3$—ST) and potassium tantalate ($KTaO_3$—KT), pure or modified, are of particular importance. They are both quantum paraelectrics with high dielectric permittivity and low losses that can find application in tunable microwave devices due to a dependence of the permittivity on the electric field. Factors as Sr/Ti and K/Ta ratio in ST and KT ceramics, respectively, can alter the defect chemistry of these materials and affect the microstructure. Therefore, if properly understood, cation stoichiometry variation may be intentionally used to tailor the electrical response of electroceramics. The scientific and technological importance of the stoichiometry variation in ST and KT ceramics is reviewed and compared in this chapter. The differences in crystallographic phase assemblage, grain size, and dielectric properties are described in detail. Although sharing crystal chemical similarities, the effect of the stoichiometry is markedly different. Even if the variation of Sr/Ti and K/Ta ratios did not change the quantum-paraelectric nature of ST and KT, Sr excess impedes the grain growth and decreases the dielectric permittivity in ST ceramics, while K excess promotes the grain growth and increases the dielectric permittivity in KT ceramics.

Keywords: nonstoichiometry, perovskite, electroceramics, ferroelectrics, crystallographic phase assemblage, grain growth, dielectric spectroscopy

1. Introduction

Considering functional oxides, ferroelectrics are essential materials, being used in a wide range of applications [1, 2]. Ferroelectrics are nonlinear dielectric materials and their main characteristic is a spontaneous electric polarisation that can exist without an external electric field and can be reversed by the application of the field [1, 3]. Ferroelectricity is a temperature-dependent property, inherent to materials with a noncentrosymmetric crystal structure that is lost above the characteristic temperature designated as Curie temperature (T_0), when the material becomes centrosymmetric and paraelectric. Although ferroelectric materials hold their main functionality in the polar state (below T_0), they are also useful above T_0, in the paraelectric state [4, 5]. In this nonpolar, phase ferroelectrics are normally characterised by a real part of the dielectric permittivity ε' (or susceptibility $\chi' = \varepsilon' - 1$), which depends on temperature, according to the Curie-Weiss law (Eq. (1)):

$$\varepsilon' \approx \chi' = C/(T - T_0), \tag{1}$$

where C is the Curie constant and T_0 is the Curie temperature, above which the ferroelectric material is in the paraelectric state [1, 3]. For a second-order phase transition, the transition temperature $T_C = T_0$, but for a first-order transition $T_C > T_0$ (see **Figure 1**). As also schematically shown in **Figure 1**, the second-order transition is characterised by a smooth increase of the spontaneous polarisation P_s as the temperature decreases starting from T_C, while for the first-order transition P_s jumps for some value at T_C with a further slight increase as temperature decreases [3].

Besides the temperature, ε' depends on the applied electric field, particularly, near the phase transition. There are two parameters used for the characterisation of the dependence of the dielectric permittivity on the applied DC bias electric field: (1) tunability n, defined as the ratio of the dielectric permittivity of the material at zero electric field to that at some nonzero electric field and (2) relative tunability n_r, defined as (Eq. (2)):

$$n_r(E) = [\varepsilon'(0) - \varepsilon'(E)]/\varepsilon'(0) = (n - 1)/n, \tag{2}$$

where $\varepsilon'(0)$ is the dielectric permittivity at zero field and $\varepsilon'(E)$ is the dielectric permittivity under the applied field E [4]. Thus, permittivity is an important parameter in defining capacitors with high capacity to store electrical energy, as well as high-performance tunable microwave devices, for example, phase shifters, as components in electronically scanned phased-array antennas for communications and radar applications because of their low dielectric losses and reasonable

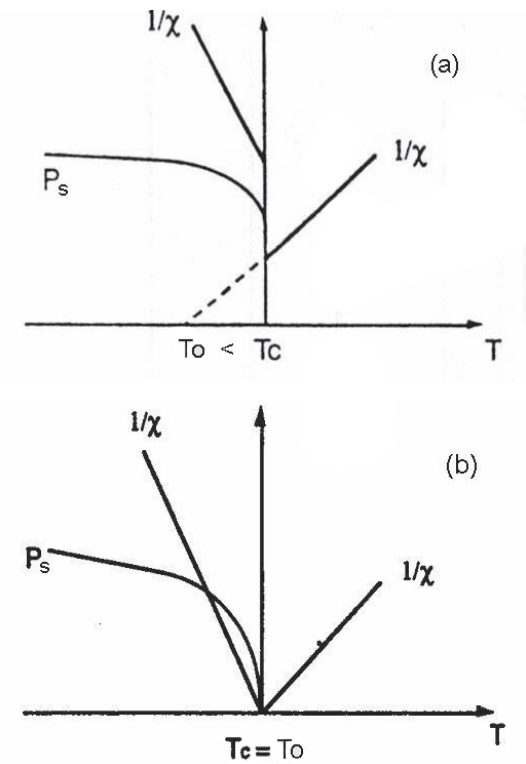

Figure 1.
Temperature dependence of inverse dielectric susceptibility χ′ and spontaneous polarisation P_s for first-order (a) and second-order (b) ferroelectric phase transitions (adapted from Smolenskii [3]).

tunability [5]. Moreover, the dielectric permittivity is a complex parameter, consisting of a real part ε' and an imaginary part ε'', while their ratio determines the dissipation factor $\tan\delta = \varepsilon''/\varepsilon'$. In this respect, incipient ferroelectrics (or quantum paraelectrics), such as perovskite type $SrTiO_3$ (ST) and $KTaO_3$ (KT), are of great interest because they do not possess the phase transition into polar phase at any temperature, simultaneously presenting very low dielectric losses. Indeed, they can possess a dissipation factor $\tan\delta$ as low as 10^{-4}–10^{-5} that is very attractive for microwave applications [6, 7].

Strontium titanate ($SrTiO_3$, ST) and potassium tantalate ($KTaO_3$, KT) belong to the family of incipient ferroelectrics because their dielectric permittivity monotonously increases upon cooling down to near 0 K without any ferroelectric-type anomaly [8]. However, since the ferroelectric order in these two materials is suppressed by quantum fluctuations, they can also be called quantum paraelectrics [9, 10], while their $\varepsilon'(T)$ dependence can be described by Barrett's relation (Eq. (3)):

$$\varepsilon'(T) = \frac{C}{\frac{T_1}{2}\coth\frac{T_1}{2T} - T_0} + \varepsilon_1 \tag{3}$$

which is based on the mean-field theory taking quantum fluctuations into account [11]. Comparing to Eq. (1) for the Curie-Weiss law, a temperature of the crossover between classical and quantum behaviour T_1 and a temperature-independent component of permittivity ε_1 are introduced in Eq. (3) for the Barrett's relation. However, in the limit $T \gg T_1$, the Barrett's relation transforms into the traditional Curie-Weiss law. The low-temperature paraelectric phase is thus unstable in quantum paraelectrics, and the ferroelectric state can be induced by the application of a high electric field [12], uniaxial stress [13], cation [10, 14–16], or oxygen isotope substitutions in the lattice [17].

Structurally, ST and KT are similar and both crystalize with a perovskite-type structure [16, 18]. The general chemical formula for the perovskite oxides is ABO_3, where A and B are cations of very different sizes (A are larger than B), and O is an oxygen that bonds to both. As shown in **Figure 2**, the perovskite unit cell is ideally cubic, where A-cations are placed at the cube corners, B-cations are located at the body centre, and the position of oxygen ions is at the centre of the faces. The cell packaging is characterised by the Goldschmidt tolerance factor (Eq. (4)):

$$t = \frac{r_A + r_O}{\sqrt{2}(r_B + r_O)} \tag{4}$$

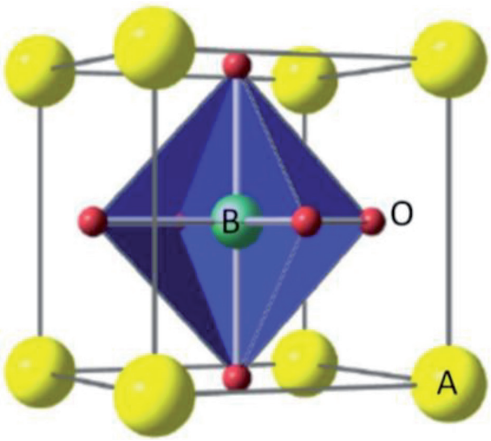

Figure 2.
Representation of the ideal cubic perovskite unit cell (ABO_3).

where r_i (i = A, B, O) denotes the average ionic radii of the constituents of ABO_3 compound in the respective sites [18, 19]. In the case of ST and KT, t is close to 1, implying that both A and B ions are closely packed and their excess solubility is very limited.

Regarding the cation excess solubility limits for the ST lattice, a presence of TiO_2 second phase was reported for ST ceramics with Ti excess down to 0.5 mol%, in agreement with similar high-temperature conductivity behaviour observed for Sr/Ti ratio ≥ 0.995 [20]. On the other hand, Sr excess is known to accommodate in the ST lattice as a three-dimensional mosaic of single-layered rock-salt blocks, forming the so-called Ruddlesden-Popper structures with the formula $SrO{\cdot}(SrTiO_3)_n$ instead of secondary phases [21]. Concerning the electrical properties, a breakdown strength was reported to be higher for ST ceramics with Sr/Ti ratio of 0.996, comparing to that for stoichiometric ones, and attributed to smaller grain size [22]. More recently, we have also investigated the effect of nonstoichiometry—Sr/Ti ratio from 0.995 to 1.02—on the high-temperature electrical response of ST ceramics, using impedance spectroscopy [23]. The resistivity of bulk and grain boundaries systematically decreased in both Ti-rich and Sr-rich ST, as compared to stoichiometric ceramics. The nonstoichiometry effect was found to be much stronger for the grain boundaries as compared to the bulk and attributed to the defect chemistry variation rather than to the microstructural development [23].

In the case of KT, in which the dielectric losses can be even lower than those of ST, thus exhibiting a dissipation factor $\tan\delta$ of ~10^{-4} in the GHz range [6, 7], stoichiometry effect is even more important and, additionally, more difficult to control due to the high volatility of the alkali element as potassium [24, 25]. As a result, the dielectric properties have been mainly reported for KT single crystals [6, 7, 10, 24, 26–29], whereas the studies on polycrystalline bulk are seldom reported [24, 25, 30], even though ceramics are simpler and less expensive to produce than single crystals. This scarcity is enhanced by the fact that although KT melts easily above 1350°C, it is hard to obtain a highly dense monophasic stoichiometric polycrystalline KT below this temperature [25]. In addition, according to our pioneer thermodynamic studies using oxide melt solution calorimetry, the enthalpy of formation of perovskite from oxides becomes less exothermic from pyrochlore phases, thus indicating a less stable structure with respect to the constituent oxides. The decomposition enthalpy of $K_2Ta_2O_6$ to $KTaO_3$ indicates that pyrochlore is energetically more stable than perovskite, and also confirms that pyrochlore is the low-temperature phase [31].

Needless to state that the optimisation of the dielectric response of functional materials is evidently associated with the precise control of the composition (namely the stoichiometry). Therefore, this chapter is aimed to overview and to compare the effect of cationic ratio on the microstructural and dielectric properties of ST and KT ceramics.

2. Experimental

2.1 Preparation of ST ceramics

Ceramics of strontium titanate were prepared by conventional mixed oxide method [32]. Reagent grades $SrCO_3$ and TiO_2 were weighed according to the compositions $Sr_{1.02}TiO_{3.02}$, $SrTiO_3$ and $Sr_{0.997}TiO_{2.997}$. After milling in alcohol for 8 h using Teflon pots and zirconia balls in a planetary mill, the powders were dried, and then calcined at 1150°C for 2 h. The calcined powders were ball milled under similar conditions as the previous ones and dried again to obtain powders with particle size

lower than 5 μm. Pellets of 10 mm in diameter were uniaxially pressed at 100 MPa and then isostatically pressed at 200 MPa. Sintering was performed in air at 1500°C for 5 h with heating and cooling rates of 5°C/min. The density of all the sintered samples, reached ~97% of the theoretical density of ST.

2.2 Preparation of KT ceramics

Ceramics of potassium tantalate were also prepared by the conventional mixed oxide method [33]. After being dried for dehydration, K_2CO_3 and Ta_2O_5 reagents were weighed according to the compositions $KTaO_3$, $K_{1.02}TaO_{3.01}$, and $K_{1.05}TiO_{3.025}$. Once milled in a planetary mill for 5 h using Teflon pots, zirconia balls, and alcohol, the powders were dried, and then calcined at 875°C for 8 h. The calcined powders were ball milled in alcohol for 5 h and dried again. Pellets of 10 mm in diameter were uniaxially pressed at 100 MPa, covered by powder of the same composition to decrease the loss of potassium, and sintered in closed alumina crucibles at 1350°C for 1 h with heating and cooling rates of 5°C/min. The density of all the sintered samples varied from ~87 to 90% of the theoretical density of KT. Through weight loss and inductively coupled plasma spectroscopy analysis, the potassium loss was about 3–4%.

2.3 Characterisation of the ceramics

Room temperature X-ray diffraction (XRD) analysis (Rigaku D/Max-B, Cu Kα) was conducted on some of the grounded sintered pellets with a scanning speed of 1 °/min and a step of 0.02°. Lattice parameters were refined by the least-square fitting to the observed XRD data, between 2Θ = 20° and 110°, using WinPLOTR software. The microstructure of the ceramics was observed on polished and thermally etched sections using scanning electron microscopy (SEM, Hitachi S-4100 and Hitachi SU-70). The average grain size of the sintered pellets was measured on at least 100 grains by AnalySIS (Soft Imaging System GmbH) software. For the dielectric measurements, gold electrodes were sputtered on both sides of the polished ceramics. The dielectric permittivity and loss were measured at different frequencies between 100 Hz and 1 MHz, using Precision LCR Meter HP 4284A and a Displex APD-Cryogenics cryostat of He closed cycle during heating in the temperature range from 10 to 300 K.

3. Results

3.1 Structure and microstructure

XRD patterns of the sintered ST ceramics with initial Sr/Ti ratio = 0.997, 1, and 1.02 are shown in **Figure 3** (left). From the XRD analysis, all ST compositions under study have a cubic perovskite structure and are monophasic. No systematic variation of the lattice parameter was observed.

For the sintered KT ceramics with initial K/Ta ratio = 1, 1.02, and 1.05, the XRD patterns are shown in **Figure 3** (right). The observed X-ray diffraction lines are consistent with the cubic perovskite symmetry of stoichiometric KT for all the precursor compositions. For ceramics with K/Ta = 1.05 and 1.02, no distinct secondary phases are detected. Conversely, additional diffraction lines observed in the patterns for K/Ta = 1, evidence the existence of a secondary phase, which was assigned to the potassium-poor tungsten bronze structure $K_6Ta_{10.8}O_{30}$ phase. These results are in agreement with an homogeneous distribution of both potassium and tantalum

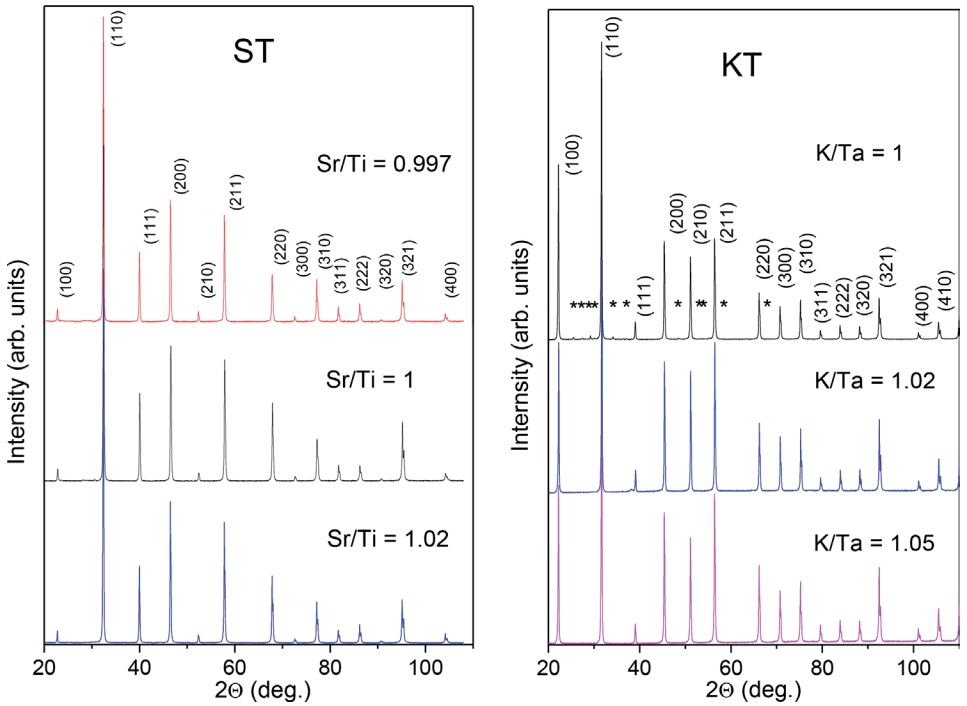

Figure 3.
*XRD patterns of sintered strontium titanate ($SrTiO_3$, ST) (left) and potassium tantalate and potassium tantalate ($KTaO_3$, KT) (right) ceramics, prepared with indicated Sr/Ti and K/Ta ratios (adapted from [32, 33]). Reflections of ST and KT phases are marked by their corresponding crystallographic indexes and reflections of $K_6Ta_{10.8}O_{30}$ secondary phase are marked by *.*

in the grains of KT ceramics with initial K/Ta ratio of 1.05 and 1.02, observed by elemental mapping using energy dispersive spectroscopy, while some Ta-rich areas were detectable in the ceramics with the initial K/Ta = 1 [33]. Moreover, since no secondary phase was detected in the XRD patterns of KT powders after calcination (not shown) for all the precursor compositions including K/Ta = 1, it is assumed that the sintering process at 1350°C mainly leads to the loss of volatile potassium. The lattice parameter values of KT phase deduced from the XRD patterns were close to that of 3.989 Å for KT single crystals [26].

Rather dense microstructures and significant difference in the grain size for Ti-rich and Sr-rich ST ceramics was observed by scanning electron microscopy [32]. The average grain size of ST ceramics with Sr/Ti ≤ 1 was found to be of about 20 μm, that is, in the range of tens of microns, whereas Sr/Ti > 1 yields ceramics with the grain size of about 6 μm, that is, in the micron range (see **Table 1**). The microstructural analysis of KT ceramics revealed cubic-like grain shape and well-defined porosity [32] in agreement with the ceramics relative density of about 88%. Moreover, the grain size was found to grow from submicron to several microns range with K/Ta ratio increasing from 1 to >1. Average grain-size values of 0.7, 4.9, and 6.5 μm were determined for the ceramics with initial K/Ta ratio of 1, 1.02, and 1.05, respectively, as also displayed in **Table 1**.

Thus, the grain-size dependence on the stoichiometry of ST and KT ceramics behaves oppositely. The larger grains are formed for excess of B-site cations in ST and for excess of A-site cations in KT. Such dissimilarity is based on the unique crystallochemistry details of each system, as displayed by their phase diagram. An eutectic liquid phase that promotes the grain growth during the sintering exists on the Ti-rich side of the SrO-TiO_2 phase diagram, when Sr/Ti < 1 [34]. In contrast,

Ceramics	A/B ratio	Average grain size, μm	ε'_{max}	$\tan\delta_{min}$, %	Barrett relation parameters			
					T_0, K	T_1, K	$C/10^3$, K	ε_1
ST	0.997	20	~7700	0.40	34	98	112	—
	1	20	~6300	0.33	35	99	92	—
	1.02	6.0	~3900	0.69	32	110	87	—
KT	1	0.7	~2250	0.34	14	66	38	123
	1.02	4.9	~4000	0.25	12	48	49	58
	1.05	6.5	~4000	0.62	10	48	57	120

Table 1.
Average grain size and Barrett's relation parameters for $SrTiO_3$, ST ceramics with initial Sr/Ti ratio of 1, 1.02, and 0.997 sintered at 1500°C for 5 h and for $KTaO_3$, KT ceramics with initial K/Ta ratio = 1, 1.02, and 1.05 sintered at 1350°C for 1 h [32, 33].

the KT grain boundaries become wet close to the eutectic temperature that emerges for K/Ta > 1 [35]. Then, grain boundary diffusion increases and grain growth is promoted in the presence of potassium excess.

3.2 Electrical properties

The low-frequency dielectric measurements data are summarised in **Figures 4** and **5**. The temperature dependence of the dielectric permittivity (ε') for stoichiometric and nonstoichiometric ST ceramics, which revealed no considerable frequency dispersion is shown in **Figure 4a** for the frequency of 10 kHz. No dielectric permittivity anomaly was observed, as well. The dielectric permittivity increases steeply and levels-off at high values as the temperature approaches 0 K, revealing a typical behaviour of quantum paraelectrics [9, 10]. Comparing with stoichiometric composition, Sr excess lowers the dielectric permittivity values at low temperatures from ~6300 to ~3900, while Ti excess raises it to ~7700, as also listed in **Table 1**. The later value is lower than that of ~20,000, reported for ST single crystals [9], due to the contribution of pores and grain boundaries with much lower permittivity than that of ST bulk [36]. However, it is much higher than that of ~5600 for conventionally prepared ST ceramics sintered at lower temperature of 1400°C [37] and even higher than that of ~6850, reported for higher purity sol-gel derived ST ceramics [38].

The temperature dependence of the dielectric permittivity of KT ceramics, with initial K/Ta ratio = 1, 1.02, and 1.05 at the frequency of 10 kHz is shown in **Figure 4b**, revealing too the continuous increase of $\varepsilon'(T)$ on cooling. The potassium excess is found to raise the dielectric permittivity monotonously in the range of initial K/Ta ratio under study, in spite of the small difference between the low-temperature dielectric permittivity for K/Ta = 1.02 and K/Ta = 1.05. For KT ceramics with initial K/Ta ratio of 1, the dielectric permittivity is about 2300. It is much smaller than that of KT single crystals [7] but close to that reported for KT ceramics [24]. Contributions of secondary phases in the ceramics, which are less polarisable than crystalline grains of KT, grain boundaries (small grain size), and pores (density ~88%) can lead to the observed permittivity decrease. On the other hand, the dielectric permittivity of similarly dense KT ceramics with initial K/Ta ratio of 1.02 and 1.05 reach a value of about 4000, which is much higher than the values, reported for K/Ta = 1 by Chen et al. [24], higher than the value of 3100, reported for K/Ta = 1.05 by Axelsson et al. [25], and is not much below 5000,

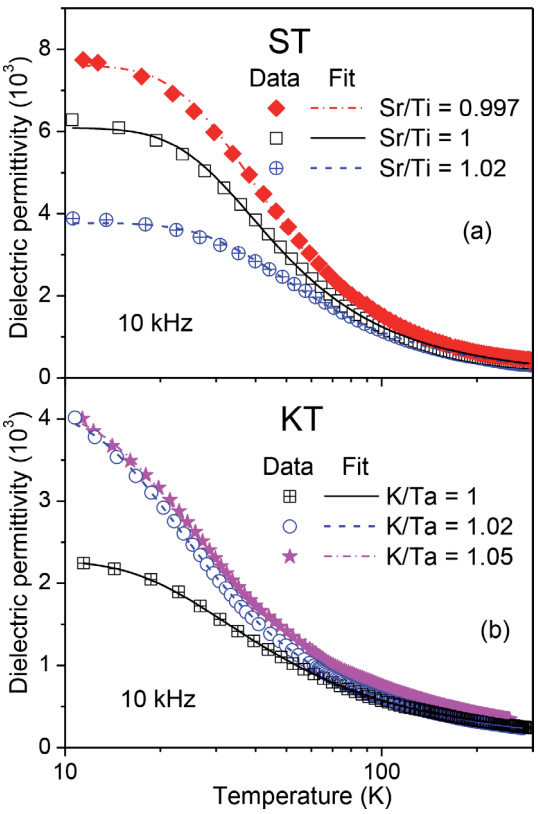

Figure 4.
Temperature dependence of the real part of the dielectric permittivity ε′ of strontium titanate ($SrTiO_3$, ST) (a) and potassium tantalate ($KTaO_3$, KT) (b) ceramics with indicated Sr/Ti and K/Ta ratios at frequency of 10 kHz (adapted from [32, 33]). The fit curves of the experimental data to the Barrett's relation are shown as well.

which was reported for KT single crystals [7]. In parallel to our work, Glinšek et al., obtained monophasic KT ceramics with relative density ≥95% using hot-pressing of mechanically activated powders at 1250°C and 25 MPa for 2 h [30]. However, the maximum permittivity of the ceramics prepared from single calcined powder was still about 2500. Just by using a double calcination, a dielectric permittivity up to 4080 and a dissipation factor between 0.001 and 0.016 at 1 kHz were reported for these dense hot-pressed KT ceramics [30].

Figure 5a presents the temperature dependence of the dielectric losses, tanδ at 10 kHz for stoichiometric and nonstoichiometric ST ceramics. For stoichiometric ST, a strong loss peak is evident at 70–105 K for the frequency range 10^2–10^6 Hz. Such a peak observed also in nominally pure ST single crystals can be attributed to the slowing down of polar modes at unavoidable defects within ferroelastic domain walls [39, 40]. ST ceramics with Sr/Ti = 1.02 show the concomitant suppression of the loss peak in contrast to the ceramics with Ti excess that have a very weak effect on the dielectric loss behaviour of ST. The minimum dissipation factor values are listed in **Table 1**.

From the temperature dependence of the dielectric loss at 10 kHz for KT ceramics with initial K/Ta ratio = 1, shown in **Figure 5b**, up to five peaks around 27, 49, 62, 127, and 214 K, can be detected. For K/Ta ratio = 1.02, similar but less intense peaks (below 0.007) are observed as well. Moreover, another low intense peak emerges at about 89 K. For K/Ta ratio = 1.05, the later peak grows, becoming

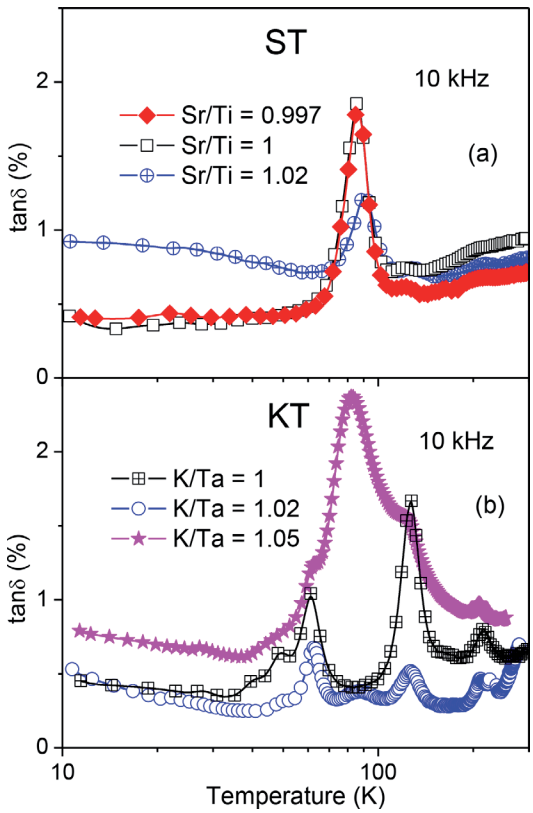

Figure 5.
Temperature dependence of the dissipation factor tanδ of strontium titanate ($SrTiO_3$, ST) (a) and potassium tantalate ($KTaO_3$, KT) (b) ceramics with indicated Sr/Ti and K/Ta ratios at frequency of 10 kHz (adapted from [32, 33]).

a dominant one and shifting to 83 K. All the other peaks mostly transform into shoulders. Therefore, potassium excess first decreases the dielectric loss down to 0.0025 (see also **Table 1**), reducing the peak intensities, but then strongly increases the loss up to 0.0237, inducing a strong peak close to 83 K. Thus, even compared with double calcined hot-pressed KT ceramics [30], close permittivity and lower losses could be obtained by conventional method just using 2% excess of potassium.

4. Analysis and discussion

The temperature dependences of the dielectric permittivity for both ST ceramics with Sr/Ti = 0997, 1, 102 and KT ceramics with K/Ta = 1, 1.02, and 1.05 were fitted by Barrett's relation (Eq. (3)). As shown in **Figure 4**, the fitting curves match well the $\varepsilon'(T)$ data points. The fitted parameters of the Barrett's relation for these experimental data are indicated in **Table 1**. T_0 values of 32–35 K for ST ceramics and of 10–14 K for KT ceramics as well as T_1 values of 98–110 and 48–66 K for ST and KT ceramics, respectively, are in agreement with those for corresponding ceramics and single crystals reported in the literature and summarised in **Table 2**.

As also seen from **Table 1**, whereas nonstoichiometry does not tend to change the transition temperature T_0 both for ST and KT, C parameter increases from 87×10^3 to 112×10^3 K with decreasing Sr/Ti ratio in ST and from 38×10^3 to

Composition	Type	T_0, K	T_1, K	$C/10^3$, K	ε_1	Ref.
$SrTiO_3$	SC	35.5	80.0	80.0	—	[9]
	CER	25.0	84.0	81.0	—	[37]
	CER	43.2	110.0	78.0	—	[38]
$KTaO_3$	SC	12.9	54.2	55.8	—	[28]
	SC	13.1	56.9	54.5	47.5	[24]
	SC	8.0	48.3	61.8	48.0	[24]
	CER	5.2	60.0	48.6	49.0	[24]
	CER	15.0	56.0	51.0	64.0	[30]

SC, single crystals; CER, ceramics.

Table 2.
Parameters of the Barrett's relation reported in literature for the quantum paraelectrics, $SrTiO_3$, ST and $KTaO_3$, KT.

57×10^3 K with increasing initial K/Ta ratio in KT ceramics. The increase of C reflects the increase of the $\varepsilon'(T)$ amplitude. In the case of KT, such increase might be explained by two reasons. On one hand, there is a strong increase of the grain size and decrease of the weak grain boundary contribution to the dielectric permittivity for K/Ta > 1. On the other hand, there is a reduction and final disappearance of the less polarisable potassium-poor secondary phase with increasing K/Ta ratio. In the case of ST, the increase of permittivity for Ti-rich ST can be related to the enhanced polarisability of the lattice, fully packed by Ti^{4+} ions. Ti^{4+} ions are the most polarisable in ST [41], while their collective off-central displacement is responsible for ferroelectricity establishment and therefore permittivity increase in titanates. On the other hand, the excess of Sr fully accommodates in the perovskite ST lattice forming interlayers within the RP structure. Such interlayers are expected to be less polarisable than the perovskite lattice [42], thus contributing to the lowering of the dielectric permittivity observed in the present work for Sr-rich ST. The reduction of the grain size in these compositions is another factor that can also contribute to such a decrease [36].

5. Conclusions

The effect of Sr/Ti ratio (0.997–1.02) and initial K/Ta ratio (1–1.05) on the phase morphology and dielectric response of ST and KT ceramics, respectively, is overviewed. Whereas no second phases were detected for the studied ST ceramics, initial excess of potassium was shown to be necessary to yield single-phase KT ceramics by solid state reaction process. Moreover, potassium excess favours the grain growth in KT ceramics, whereas Sr excess impedes the grain growth in ST ceramics and thus decreases the dielectric permittivity. On the contrary, Ti excess promotes the increase of the dielectric permittivity values of ST ceramics. Combination of the absence of secondary phases with increased grain size in KT ceramics with initial potassium excess results simultaneously in the increase of the lowest temperature dielectric permittivity value. Furthermore, the variation of Sr/Ti and K/Ta ratios did not change the quantum-paraelectric nature of ST and KT, respectively. Fitting the Barrett's relation to the experimental data revealed just considerable dissimilarities in the Curie-Weiss constants in agreement with the highest permittivity variation with A/B ratios, while characteristic temperatures did not change significantly.

Acknowledgements

This work was developed within the scope of the project CICECO-Aveiro Institute of Materials, FCT Ref. UID/CTM/50011/2019, financed by national funds through the FCT/MCTES.

Author details

Alexander Tkach and Paula M. Vilarinho*
Department of Materials and Ceramic Engineering, CICECO—Aveiro Institute of Materials, University of Aveiro, Aveiro, Portugal

*Address all correspondence to: paula.vilarinho@ua.pt

References

[1] Vilarinho PM. Functional materials: Properties, processing and applications. In: Vilarinho PM, Rosenwaks Y, Kingon A, editors. Scanning Probe Microscopy: Characterization, Nanofabrication and Device Application of Functional Materials. Dordrecht: Kluwer Academic Publishers; 2005. pp. 3-33

[2] Martin LW, Rappe AM. Thin-film ferroelectric materials and their applications. Nature Reviews Materials. 2016;**2**:16087

[3] Smolenskii GA, editor. Ferroelectrics and Related Materials. New York: Gordon and Breach Science Publishers; 1984

[4] Tagantsev AK, Sherman VO, Astafiev KF, Venkatesh J, Setter N. Ferroelectric materials for microwave tunable applications. Journal of Electroceramics. 2003;**11**:5-66

[5] Gevorgian S. Introduction: Overview of agile microwave technologies. In: Gevorgian S, editor. Ferroelectrics in Microwave Devices, Circuits and Systems. London: Springer Publishing; 2009. pp. 1-19

[6] Vendik OG, Ter-Martirisian LT, Zubko SP. Microwave losses in incipient ferroelectrics as functions of the temperature and the biasing field. Journal of Applied Physics. 1998;**84**:993-998

[7] Geyer RG, Riddle B, Krupka J, Boatner LA. Microwave dielectric properties of single-crystal quantum paraelectrics $KTaO_3$ and $SrTiO_3$ at cryogenic temperatures. Journal of Applied Physics. 2005;**97**:104111

[8] Lemanov VV, Sotnikov AV, Smirnova EP, Weihnacht M, Kunze R. Perovskite $CaTiO_3$ as an incipient ferroelectric. Solid State Communications. 1999;**110**:611-614

[9] Müller KA, Burkard H. $SrTiO_3$: An intrinsic quantum paraelectric below 4 K. Physical Review B. 1979;**19**:3593-3602

[10] Samara GA. The relaxational properties of compositionally disordered ABO_3 perovskites. Journal of Physics: Condensed Matter. 2003;**15**:R367-R411

[11] Barrett JH. Dielectric constant in perovskite type crystals. Physics Review. 1952;**86**:118-120

[12] Fleury PA, Scott JF, Worlock JM. Soft phonon modes and the 110°K phase transition in $SrTiO_3$. Physical Review Letters. 1968;**21**:16-19

[13] Uwe H, Sakudo T. Stress-induced ferroelectricity and soft phonon modes in $SrTiO_3$. Physical Review B. 1976;**13**:271-286

[14] Lemanov VV. Phase transitions in $SrTiO_3$ quantum paraelectric with impurities. Ferroelectrics. 1999;**226**:133-146

[15] Tkach A, Vilarinho PM, Kholkin AL. Polar behavior in Mn-doped $SrTiO_3$ ceramics. Applied Physics Letters. 2005;**86**:172902

[16] Levin I, Krayzman V, Woicik JC, Tkach A, Vilarinho PM. X-ray absorption fine structure studies of Mn coordination in doped perovskite $SrTiO_3$. Applied Physics Letters. 2010;**96**:052904

[17] Itoh M, Wang R, Inaguma Y, Yamaguchi T, Shan Y-J, Nakamura T. Ferroelectricity induced by oxygen isotope exchange in strontium titanate perovskite. Physical Review Letters. 1999;**82**:3540-3543

[18] Bhalla AS, Guo RY, Roy R. The perovskite structure—A review of its

role in ceramic science and technology. Materials Research Innovations. 2000;**4**:3-26

[19] Goldschmidt VM. Geochemisce verterlungsgesetze der elemente. Oslo: Norske Videnskap; 1927

[20] Witek S, Smyth DM, Pickup H. Variability of the Sr/Ti ratio in $SrTiO_3$. Journal of the American Ceramic Society. 1984;**67**:372-375

[21] Balachandran U, Eror NG. On the defect structure of strontium-titanate with excess SrO. Journal of Materials Science. 1982;**17**:2133-2140

[22] Wang Z, Caon M, Yaon Z, Li G, Song Z, Hu W, et al. Effects of Sr/Ti ratio on the microstructure and energy storage properties of nonstoichiometric $SrTiO_3$ ceramics. Ceramics International. 2014;**40**:929-933

[23] Amaral L, Tkach A, Vilarinho PM, Senos AMR. New insights into the effect of nonstoichiometry on the electric response of strontium titanate ceramics. Journal of Physical Chemistry C. 2019;**123**:710-718

[24] Chen ZX, Zhang XL, Cross LE. Low-temperature dielectric properties of ceramic potassium tantalate ($KTaO_3$). Journal of the American Ceramic Society. 1983;**66**:511-515

[25] Axelsson A-K, Pan Y, Valant M, Alford N. Synthesis, sintering and microwave dielectric properties of $KTaO_3$ ceramics. Journal of the American Ceramic Society. 2009;**92**:1773-1778

[26] Davis TG. Dielectric properties and soft modes in the ferroelectric mixed crystals $K_{1-x}Na_xTaO_3$. Physical Review B. 1972;**5**:2530-2537

[27] Samara GA, Morosin B. Anharmonic effects in $KTaO_3$-ferroelectric mode, thermal-expansion, and compressibility. Physical Review B. 1973;**8**:1256-1264

[28] Vogt H, Uwe H. Hyper-Raman scattering from the incipient ferroelectric $KTaO_3$. Physical Review B. 1984;**29**:1030-1034

[29] Zlotnik S, Vilarinho PM, Costa MEV, Moreira JA, Almeida A. Growth of incipient ferroelectric $KTaO_3$ single crystals by a modified self-flux solution method. Crystal Growth and Design. 2010;**10**(8):3397-3404

[30] Glinšek S, Malič B, Rojac T, Filipič C, Budič B, Kosec M. $KTaO_3$ ceramics prepared by the mechanochemically activated solid-state synthesis. Journal of the American Ceramic Society. 2011;**94**:1368-1373

[31] Zlotnik S, Sahu SK, Navrotsky A, Vilarinho PM. Pyrochlore and perovskite potassium tantalate: Enthalpies of formation and phase transformation. Chemistry—A European Journal. 2015;**21**:5231-5237

[32] Tkach A, Vilarinho PM, Senos AMR, Kholkin AL. Effect of nonstoichiometry on the microstructure and dielectric properties of strontium titanate ceramics. Journal of the European Ceramic Society. 2005;**25**:2769-2772

[33] Tkach A, Vilarinho PM, Almeida A. Role of initial potassium excess on the properties of potassium tantalate ceramics. Journal of the European Ceramic Society. 2011;**31**:2303-2308

[34] Levin EM, Robbins CR, McMurdie HF. Phase Diagrams for Ceramists. Columbus: The American Ceramic Society; 1964

[35] Reisman A, Holtzberg F, Berkenblit M, Berry M. Reactions of the group VB pentoxides with alkali

oxides and carbonates. III. Thermal and X-ray phase diagrams of the system K_2O or K_2CO_3 with Ta_2O_5. Journal of the American Chemical Society. 1956;**78**:4514-4520

[36] Petzelt J, Ostapchuk T, Gregora I, Rychetský I, Hoffmann-Eifert S, Pronin AV, et al. Dielectric, infrared, and Raman response of undoped $SrTiO_3$ ceramics: Evidence of polar grain boundaries. Physical Review B. 2001;**64**:184111

[37] Yu Z, Ang C. Dielectric and conduction behavior of La-doped $SrTiO_3$ with suppressed quantum-paraelectric background. Applied Physics Letters. 2002;**80**:643-645

[38] Tkach A, Okhay O, Vilarinho PM, Kholkin AL. High dielectric constant and tunability of strontium titanate ceramics modified by chromium doping. Journal of Physics: Condensed Matter. 2008;**20**:415224

[39] Viana R, Lunkenheimer P, Hemberger J, Bohmer R, Loidl A. Dielectric spectroscopy in $SrTiO_3$. Physical Review B. 1994;**50**: 601-604

[40] Ang C, Guo R, Bhalla AS, Cross LE. Effect of electric field and post-treatment on dielectric behavior of $SrTiO_3$ single crystal. Journal of Applied Physics. 2000;**87**:3937-3940

[41] Shannon RD. Dielectric polarizabilities of ions in oxides and fluorides. Journal of Applied Physics. 1993;**73**:348-366

[42] Wise PL, Reaney IM, Lee WE, Iddles DM, Cannell DS, Price TJ. Tunability of τ_f in perovskites and related compounds. Journal of Materials Research. 2002;**17**:2033-2040